A unified drain current $1/f$ noise model for GaN-based high electron mobility transistors*

Liu Yu-An(刘宇安), Zhuang Yi-Qi(庄奕琪)†, Ma Xiao-Hua(马晓华), Du Ming(杜 鸣), Bao Jun-Lin(包军林), and Li Cong(李 聪)

School of Microelectronics, Xidian University , Xi'an 710071, *China*

(Received 14 January 2013; revised manuscript received 13 May 2013; published online 10 December 2013)

In this work, we present a theoretical and experimental study on the drain current $1/f$ noise in the AlGaN/GaN high electron mobility transistor (HEMT). Based on both mobility fluctuation and carrier number fluctuation in a two-dimensional electron gas (2DEG) channel of AlGaN/GaN HEMT, a unified drain current $1/f$ noise model containing a piezoelectric polarization effect and hot carrier effect is built. The drain current $1/f$ noise induced by the piezoelectric polarization effect is distinguished from that induced by the hot carrier effect through experiments and simulations. The simulation results are in good agreement with the experimental results. Experiments show that after hot carrier injection, the drain current $1/f$ noise increases four orders of magnitude and the electrical parameter degradation $\Delta g_{\rm m}/g_{\rm m}$ reaches 54.9%. The drain current $1/f$ noise degradation induced by the piezoelectric effect reaches one order of magnitude; the electrical parameter degradation $\Delta g_{\rm m}/g_{\rm m}$ is 11.8%. This indicates that drain current $1/f$ noise of the GaN-based HEMT device is sensitive to the hot carrier effect and piezoelectric effect. This study provides a useful reliability characterization tool for the AlGaN/GaN HEMTs.

Keywords: $1/f$ noise, hot carrier, piezoelectric effects, AlGaN/GaN, HEMT

PACS: 07.50.Hp, 85.40.Hp, 71.55.Eq **DOI:** 10.1088/1674-1056/23/2/020701

1. Introduction

After more than a decade of research, GaN-based high electron mobility transistors (HEMTs) provide advantages for power amplifier design, which may be used in areas of radar, cellular base stations and satellite. However, their performances are still restricted by frequency-dependent dispersion mechanisms and permanent degradation mechanisms, which act as the detriment of the predicted and long-term power performances.[1] Low frequency noise (LFN) in HEMT is important since it becomes an important limitation of the device performances. These mechanisms originate either from trapping-detrapping processes in surface states and deep traps associated with material quality induced by piezoelectric polarization effects[2,3] or from permanent degradation induced by hot carrier interaction with trap sites occurring in the gate-drain region.[4] Although in as early as 1998, Balandin *et al.*[5] measured the GaN-based HEMTs $1/f$ noise. Later, for characterizing various kinds of reliability problems of the GaN-based HEMT device, Vertiatchikh and Eastman,[6] Rao and Bosman[7] and Vitusevich *et al.*[8] established $1/f$ noise models independently. All of their studies are based on the Hooge carrier mobility fluctuation model. Also, in their $1/f$ noise models of the intrinsic defect, the stress situation was not considered. Manouchehri *et al.*[9] studied the AlGaN/GaN HEMT $1/f$ noise model based on non-fundamental low frequency noise theory. In nature, it is a GaN-based HEMT $1/f$ noise model based on the mobility fluctuation incorporation of the piezoelectric effects. For the serious failure modes of hot carrier effects, very little is known about the $1/f$ noise degradation model caused by the hot-carrier effect in GaN-based HEMTs. Therefore, there is an urgent need to establish a new noise model that contains the hot carrier effect. For this problem, combining the actual working conditions of the device (the operating conditions of the device refer to the room temperature and switch conversion), we present a unified theoretical model for the drain current $1/f$ noise based on both the mobility fluctuation and carrier number fluctuation in the two-dimensional electron gas (2DEG) channel of AlGaN/GaN HEMT, in which the hot carrier effect and piezoelectric effect are considered. Through experiments and simulations, the drain current $1/f$ noise induced by the piezoelectric polarization effect can be distinguished from the hot carrier effect. Those results may provide a useful reliability characterization tool for the AlGaN/GaN HEMTs.

2. Modeling

A number of contradictive approaches have so far been adopted in modeling the $1/f$ low frequency noise of electronic devices. Among these, a model proposed by Hooge[6,7] suggests that the LFN primarily originates from the carrier mobility fluctuation. An alternative model proposed by McWhorter *et al.*[9] suggests that the $1/f$ LFN is due to the carrier trapping and de-trapping in a localized or a distributed band of trap

*Project supported by the National Natural Science Foundation of China (Grant Nos. 61076101, 61204092, 61334002, and JJ0500102508).

†Corresponding author. E-mail: yqzhuang@xidian.edu.cn

© 2014 Chinese Physical Society and IOP Publishing Ltd

sites.

In our approach, a unified theoretical model for the hot carrier-induced drain current $1/f$ noise based on the mobility fluctuation and the carrier number fluctuations is proposed. There are three cases considered in our model

Case 1 in which for a fresh device, only the background $1/f$ noise is considered, which means that the scattering of intrinsic defects from the carrier leads to the mobility fluctuation of the device. Drain current $1/f$ noise S_{I_D} can be written as[6]

$$S_{I_D} = \frac{I_D^2}{f} \cdot \frac{\alpha_H}{N}, \tag{1}$$

where I_D is the channel current, f the frequency, α_H the Hooge parameter and N the channel carrier number of the unit area. The Hooge parameter reflects the process defects in the device. As the Hooge parameter increases, more process defects are produced in the device

Case 2 in which, for a device after piezoelectric stress, drain current $1/f$ noise is superimposed by RTN noise (induced by carrier trapping-detrapping processes of piezoelectric-induced surface states and deep traps) and background $1/f$ noise. It can be written as[10]

$$S_{I_D} = \left(\frac{I_D^2}{WL}\right)\left(\frac{R}{N} + \alpha\mu\right)^2 S_{N_t}, \tag{2}$$

where I_D is the channel current, W the channel width, L the channel length, μ the channel carrier mobility, N the channel carrier number of the unit area, N_t the trap density in the unit area of the oxide layer, α the scattering coefficient of the trap charge and R the change number of channel carriers caused by unit trap. Since I_D^2/WL is a constant, the first item R/N represents the carrier number fluctuation in the device and the second item $\alpha\mu$ represents the mobility fluctuations in the device. The carriers number fluctuation is deemed to be caused by the trapping/de-trapping of the 2DEG electrons from acceptor-type trap centers located in the buffer layer; each trap causes a random telegraph noise (RTN).[9] Thus the power spectrum density (PSD) is given by

$$S_{N_t}(f) = 4\sum_i \Delta N_i^2 \frac{\tau_i}{1 + 4\pi^2 f^2 \tau_i^2}, \tag{3}$$

where $S_{N_t}(f)$ is the noise power spectrum density due to the carrier fluctuation, ΔN_i^2 the variance of the carrier fluctuation, τ_i the time constant assigned to each trap level and f the frequency.

We consider a trap level with the density N_T inside the buffer layer. We define $n_0(y,E) = N_T(y,E) \cdot f_t$, where $n_0(y,E)$ is the density of filled traps and f_t is the Fermi distribution function of the trapped levels.[9] The time-in-high-current-level, τ_H, is simply the time when the trap is empty (the capture time is denoted by τ_c). Similarly, the time-in-low-current-level τ_L, is the time when the trap is filled (the emission time is represented by τ_e).

From Shockley–Read–Hall (SRH) statistics, the mean capture and emission times corresponding to a single active trap are given by[11]

$$\tau_c = \frac{1}{\sigma(x_t) v_{th} n}, \tag{4}$$

$$\tau_e = \frac{\exp[(E_F - E_T)/kT]}{g\sigma(x_t) v_{th} n}, \tag{5}$$

where v_{th} is the average thermal velocity of the carriers, $\sigma(x_t)$ the average capture cross section of an electron trap localized at a distance x_t the distance of electron trap to the edge of the active region, g the degeneracy factor, n the number of channel free carriers, E_T the trap energy and E_F the Fermi level. In the emission time constant equation, the capture cross section can be expressed as

$$\sigma(x_t) = \sigma_0 \exp\left(-\frac{\Delta E_B}{kT}\right)\exp\left(-\frac{x_t}{\lambda_t}\right), \tag{6}$$

where σ_0 is the cross-section pre-factor, ΔE_B the barrier energy for carrier capture and λ_t the attenuation wave function coefficient. To study the behaviors of traps on the edges of the active region, one can analyze the bias voltage dependences of the capture and emission times. Level 1 represents the trap that is filled and level 2 represents the trap that is empty.

From the principle of detailed balance, one can write the ratio of the mean emission time $\langle\tau_e\rangle$ to the mean capture time $\langle\tau_c\rangle$ as[11]

$$\frac{\langle\tau_c\rangle}{\langle\tau_e\rangle} = g\exp\left(\frac{E_T - E_F}{kT}\right). \tag{7}$$

The 2DEG concentration n is calculated with respect that the lower edge of the conduction band of GaN is at the hetero-interface. Starting from an initial position assumed at the Fermi level (the lower edge of the conduction band of GaN at the hetero-interface), the following equation is used:[9]

$$n = \frac{\rho_x}{e} - \left(\frac{\varepsilon_0\varepsilon_x}{(d_{AlGaN})^2}\right)[e\phi_{bx}(\text{eff}) + E_{Fx} - \Delta E_{Cx}], \tag{8}$$

where ρ_x is polarization-induced 2DEG charge density at the polar AlGaN/GaN hetero-interface, e the electron charge, ε_x the relative dielectric constant of AlGaN, d_{AlGaN} the thickness of the barrier, $\phi_{bx(\text{eff})}$ the effective height of the Schottky barrier and ΔE_{Cx} the conduction band discontinuity at the hetero-interface. Subscript x shows all the values, each of which is a function of the Al mole fraction. It should be mentioned that in the non-ideal case, due to the existence of the surface states, effective Schottky barrier can be quite independent of Al mole fraction. If a band of continuous trap levels is considered, Eq. (1) can be written as

$$S_N(f) = \int_0^{L_g}\int_{E_V}^{E_C} \frac{4\Delta N^2(E,y)\tau h(\tau)}{1 + 4\pi^2 f^2}\,\mathrm{d}E\,\mathrm{d}y, \tag{9}$$

where L_g is the gate length, $h(\tau)$ the distribution function of the carrier lifetime, which is not a specific function of τ and

can be assumed to be in any form to have a variety of different profiles, E_V and E_C are the valence and conduction band energy levels of GaN.

$$S_{I_D} = \left(\frac{I_D^2}{WL}\right)\left(\frac{R}{N}+\alpha\mu\right)^2 \times \int_0^{L_g}\int_{E_V}^{E_C}\frac{4\Delta N^2(E,y)\tau h(\tau)}{1+4\pi^2 f^2}\,\mathrm{d}E\,\mathrm{d}y. \quad (10)$$

Case 3 in which for a device after hot carrier stress, drain current $1/f$ noise is superimposed by RTS noise (induced by carrier trapping-detrapping processes of both piezoelectric effects and hot carrier effects) and background $1/f$ noise. The time constant of the charge fluctuation can be calculated based on hot carrier induced trap model,[12] $(\tau_i)^{-1} = (\tau_c)^{-1} + (\tau_e)^{-1}$. The ratio τ_c/τ_e is related to the trap energy relative to the Fermi energy level, $E_T - E_F$ and degeneracy factor g,

$$\frac{\tau_c}{\tau_e} = \frac{\langle\tau_H\rangle}{\langle\tau_T\rangle} = g\exp\left[-(E_{cox}-E_T - \Phi_{AlGaN} + \frac{z}{T_{ox}}qV_g)/KT\right], \quad (11)$$

where E_{cox} is the oxide conduction band energy, Φ_{AlGaN} the height of AlGaN barriers, V_g the gate voltage, T_{ox} the gate oxide thickness and z the distance between the trap and the interface.

$$\tau_c = 1/\sigma n\bar{v} = \tau_{c0}\exp(E_a/KT), \quad (12)$$

where σ is the capture section of carriers, $\bar{v}$ the carrier average speed of thermal motion, n the 2DEG concentration, τ_{c0} the inverse phonon frequency and E_a the activation energy. Applying this information to Eq. (5), the noise power spectral density can be calculated as

$$S_N(f) = 4W\int_0^{L_g}\int_{E_V}^{E_C}\frac{N_T(E,y)h(y,E)\exp\left(\frac{e(E_t-E_{Fnt})}{KT}\right)\cdot\sigma n\bar{v}}{\{[\sigma n\bar{v}]^2+4\pi^2 f^2\}\cdot\left[1+\exp\left(\frac{e(E_t-E_{Fnt})}{KT}\right)\right]}\,\mathrm{d}E\,\mathrm{d}y, \quad (13)$$

where E_{Fnt} is the quasi Fermi level of the trap sites and E_t is the trap energy level. It is worth noting that only trap centers located within a few KT of E_{Fnt} are responsible for the G-R process leading to $1/f$ LFN characteristic. Trap centers far from $E_{Fnt}(|E_t - E_{Fnt}| > 2KT)$ are always either empty or occupied and therefore will not have a significant contribution to G-R noise. Applying this information to Eq. (2), the noise power spectral density can be calculated as

$$S_{I_D} = \left(\frac{I_D^2}{WL}\right)\left(\frac{R}{N}+\alpha\mu\right)^2\cdot 4W\int_0^{L_g}\int_{E_V}^{E_C}\frac{N_T(E,y)h(y,E)\exp\left(\frac{e(E_t-E_{Fnt})}{KT}\right)\cdot\sigma n\bar{v}}{\{[\sigma n\bar{v}]^2+4\pi^2 f^2\}\cdot\left[1+\exp\left(\frac{e(E_t-E_{Fnt})}{KT}\right)\right]}\,\mathrm{d}E\,\mathrm{d}y. \quad (14)$$

3. Experiment

3.1. Device for test

The device for test consists of a 200-nm GaN buffer layer and a 20-nm $Al_{0.3}Ga_{0.7}N$ layer that is grown on a high-resistivity SiC substrate by metal–organic chemical vapor deposition (MOCVD). A Schottky gate contact of Ni/Au (20-nm/20 nm) is formed by electron beam evaporation. Ohmic contacts of the Ti/Al/Ni/Au (20 nm/120 nm/55 nm/45 nm) are created for drain and source regions by electron beam evaporation.

The transistor has a gate width of 100 μm and gate length of 0.6 μm. Device structure and the motion of the stress-produced carrier are shown in Fig. 1. Under piezoelectric stress, piezoelectric charges are generated (including the positive surface charges and the charges of piezoelectric electrons).

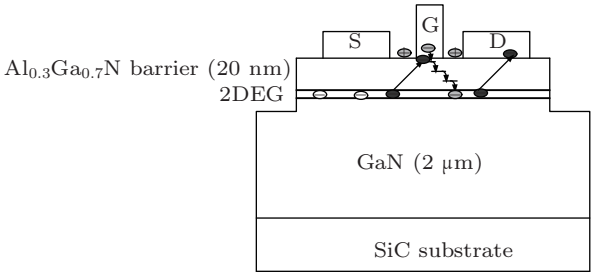


Fig. 1. Device structure and the motion of the stress-produced carriers, where S and D represent the device's source drain and G refers to the gate. The empty white circles represent channel electrons. The solid gray circles represent the piezoelectric charges (positive surface charges and the charges of electrons from the channel to the buffer layer) and the arrow indicates the direction of their motion from the gate to the channel. The solid black circles represent the hot electrons, the arrow indicates the direction of their motion from the channel to the drain.

Piezoelectric electrons are injected from the gate into the channel. Under the hot carrier stress, channel hot electrons are injected from the channel through the barrier of the buffer layer into the drain.

3.2. Hot carrier stress experiment

Devices are tested in the "ON-stress" ($V_{DS} = 10$ V, $V_{GS} = -2$ V, after 10 h), with high drain–current flow and high electric field at the same time.[4] In "ON" bias conditions, a substantial fraction of channel electrons reach sufficient energies to give rise to hot carrier effects, such as light emitting and trap generation, with consequent significant transconductance g_m degradation. After stress, there is hot electron injection to the drain, the internal electric field becomes high enough to ionize donor states at the surface, which cause selectrons to drift toward the AlGaN/GaN interface.

3.3. Piezoelectric stress experiments

Devices are tested in the "OFF-state" ($V_{GS} = -5$ V and $V_{DS} = 0.1$V, after 10 h) with high inverse gate voltage and low drain–current. In the "OFF " bias condition, it has been found that electrically active defects are generated in the AlGaN barrier or its surface in the vicinity of the gate edge. These defects are produced by the inverse piezoelectric effect introduced mechanical stress in the AlGaN barrier layer. They will become a pathway of electron flow from the gate down to the channel. It will result in trap generation and charge trapping, with a consequent decrease in I_{DSS}, g_m and an increase in drain resistance R_D and gate leakage current.[4]

3.4. Electrical parameter test

We use the semiconductor parameter analyzer HP4156B to measure the electronic parameters $g_m - V_{gs}$ of the device before and after hot carrier injection and piezoelectric effects.

3.5. $1/f$ noise parameter test

Drain–current $1/f$ noises of all devices are measured by a noise testing and analyzing system of electronic device based on a virtual instrument, which is developed in our laboratory. It includes four parts, i.e., bias circuits, low-noise preamplifier, data acquisition card and microcomputer.

The source and drain of the device are grounded, which means $V_s = V_b = 0$ V. All tests are carried out in a shield room at room temperature. The stress experiments separate from the noise test. The device operates in the linear region in noise measurement, while it operates in the cut-off region in stress measurement.

4. Results and analysis

At first, the test results of the electrical parameters are used to verify the correctness of the experiment. Then, the noise experimental results are analyzed and explained.

4.1. Results analysis of electrical parameter degradation

In general, piezoelectric effects and hot carrier effects are characterized by electrical parameter degradation.[8,13] In order to facilitate a comparison, the AlGaN/GaN HEMT hot carrier effect is characterized by electrical parameter transconductance degradation $\Delta g_m/g_m$, which is the same as the piezoelectric effect. These degradations are caused by the stress-generated defects. The defects trapping-detrapping process in surface states and deep trap influence on transconductance can be expressed as[14]

$$\frac{\Delta g_m}{g_m} = -\frac{a\mu_0}{1 + aN_t\mu_0}N_t, \tag{15}$$

where N_t is the trap number varied by the hot carrier effect or the piezoelectric effect, μ_0 is the mobility before stress, a is the empirical constant and the variation of transconductance $\Delta g_m/g_m$ is related to the number of traps N_t. As N_t increases, the variation of transconductance decreases.

4.1.1. Hot carrier-induced electronic parameter degradation

As is shown in Fig. 2, before stress $g_{m(max)}$ is 306 mS/mm, after hot carrier stress ($V_{ds} = 10$ V, $V_{gs} = -2$ V, after 10 h), $g_{m(max)}$ decreases to 138 mS/mm and the rate of change $\Delta g_m/g_m$ is 54.9%. This result is similar to that in Ref. [14].

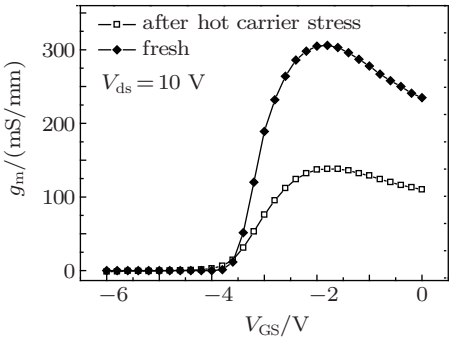


Fig. 2. Transconductances before and after hot carrier stress. The curve of fresh device is denoted by black solid square and that after stress is represented with white hollow squares.

4.1.2. Piezoelectric-induced electronic parameter degradation

As shown in Fig. 3, before stress $g_{m(max)}$ is 306 mS/mm, after piezoelectric stress ($V_{GS} = -5$ V and $V_{DS} = 0.1$ V, after 10 h), $g_{m(max)}$ decreases to 270 mS/mm, and the rate of change $\Delta g_m/g_m$ is 11.8%. This result is similar to that in Ref. [4]. Here, the correctness of piezoelectric stress and the hot carrier stress experiments are verified by electrical parameter degradation.

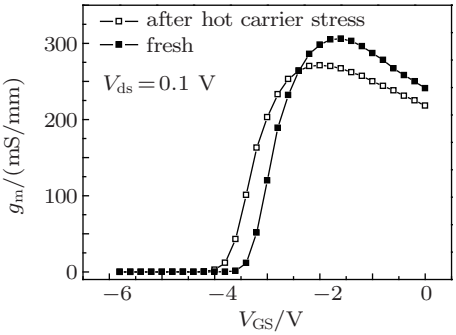


Fig. 3. Transconductances before and after piezoelectric stress. The curve of a fresh device is denoted by black solid squares and those after stress are represented with white hollow squares.

4.2. $1/f$ noise tests and simulation results

We make a comparison between simulation results and experimental data to verify the correctness of the above model. Experimental and simulation results, i.e., drain current $1/f$ noise PSD before and after hot carrier effects and piezoelectric effects, are shown in Fig. 4.

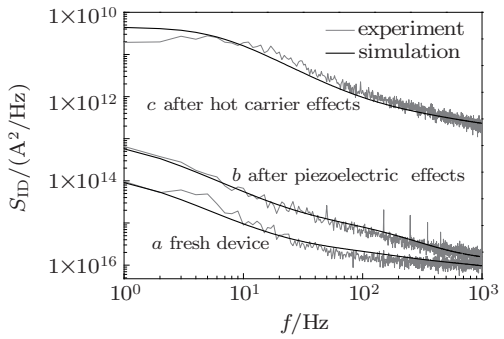


Fig. 4. Experimental and simulation results of hot carrier and piezoelectric polarization effects induced drain current $1/f$ noise PSD, where the gray line denotes the measured data, the black line represents the simulation results.

Case 1) For a fresh device, drain current $1/f$ noise complies with formula (1), there is only the background $1/f$ noise caused by the mobility fluctuation of channel carrier (as shown by empty white circles in Fig. 5). The simulation results and experimental data are shown by curve a in Fig. 4, where the gray line shows the measured data and the black line represents the simulation result. Most parts of these two curves coincide with each other.

Case 2) For a device after piezoelectric stress, drain current $1/f$ noise complies with formula (10). It is superimposed by RTN noise and background $1/f$ noise, where RTN noise is induced by carrier trapping–detrapping processes of piezoelectric-induced surface states and deep traps (as shown by the solid gray circle in Fig. 5; the arrows indicate the motion direction of hot carriers or carriers produced by piezoelectric stress from the gate to the channel). The simulation results and experimental data are shown by curve b in Fig. 4, where the gray line shows the measured data and the black line represents the simulation result. Most parts of these two curves coincide with each other.

Case 3) For a device after hot carrier stress, drain current $1/f$ noise complies with formula (14), which is superimposed by RTS noise and background $1/f$ noise. Here, RTS noise is induced by carrier trapping–detrapping processes of both the piezoelectric effect and hot carrier effect (as shown by the solid black circle in Fig. 5; arrows indicate the motion direction of hot carriers or carriers produced by piezoelectric stress from the channel to the drain). The simulation results and experimental data are shown by curve c in Fig. 4, where the gray line shows the measured data and the black line represents the simulation result. Most parts of these two curves coincide with each other.

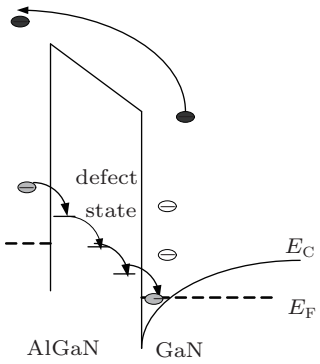


Fig. 5. Conduction band diagram of the cross section of the gate–drain edge where E_C is the conduction band energy level of GaN and E_F is the Fermi level. The empty white circle represents the channel electron. The solid gray circle represents the piezoelectric charge (positive surface charge and the charge of electrons from the channel to the buffer layer) and the arrow indicates the direction of their motion from the gate to the channel. The solid black circle represents the hot electron; the arrow indicates the direction of their motion from the channel to the drain.

The simulation is carried out using MATLAB software, based on the multi-parameter $1/f$ noise model. Simulation parameters are used as follows: trap density, oxide conduction band energy $E_{cox} = -0.5$ eV, height of the AlGaN barrier $\Phi_{AlGaN} = 1.12$ eV, capture section of carriers $\sigma = 10^{-15}$, 2DEG concentration $n = 1.2 \times 10^{13}$, activation energy $E_a = 0.201$ eV and polarization-induced 2DEG charge density $\rho_x = 1 \times 10^{12}$ cm^{-2}.

According to the experimental results, the influences of device electrical parameters and noise parameters of piezoelectric stress and hot carrier stress are specifically analyzed. Table 1 shows drain current $1/f$ noise PSDs of a fresh device before and after piezoelectric and hot carrier stress. Before and after piezoelectric stress, $1/f$ noise amplitude S_{ID} at 1 Hz increases from 9.70604×10^{-15} to 6.54055×10^{-14}; the rate of change is 574.2%. The $1/f$ noise amplitude S_{ID} at 10 Hz increases from 8.8885×10^{-16} to 6.6372×10^{-15}; the rate of change is 645.7%. The $1/f$ noise amplitude S_{ID} at 100 Hz

increases from 1.61845×10^{-16} to 6.62444×10^{-16}; the rate of change is 313.7%. The $1/f$ noise amplitude $S_{\rm ID}$ at 1000 Hz from 9.78821×10^{-17} to 1.85634×10^{-16}; the rate of change is 88.9%. Before and after hot carrier stress, $1/f$ noise amplitude $S_{\rm ID}$ at 1 Hz increases from 9.70604×10^{-15} to 1.9372×10^{-11}; the rate of change is 199610.6%. The $1/f$ noise amplitude $S_{\rm ID}$ at 10 Hz increases from 8.88851×10^{-16} to 1.90698×10^{-11}; the rate of change is 214257.4%. The $1/f$ noise amplitude $S_{\rm ID}$ at 100 Hz increases from 1.61845×10^{-16} to 1.39455×10^{-12}; the rate of change is 87146.2%. The $1/f$ noise amplitude $S_{\rm ID}$ at 1000 Hz from 9.78821×10^{-17} to 1.88307×10^{-13}; the rate of change is 19223.9%.

Table 1. Drain current $1/f$ noises before and after hot carrier and piezoelectric stress.

$S_{\rm ID}/({\rm A}^2/{\rm Hz})$	Fresh	Piezoelectric	Hot carrier
1 Hz	9.70604×10^{-15}	6.54055×10^{-14}	1.9372×10^{-11}
10 Hz	8.88851×10^{-16}	6.6372×10^{-15}	1.90698×10^{-11}
100 Hz	1.61845×10^{-16}	6.62444×10^{-16}	1.39455×10^{-12}
1000 Hz	9.78821×10^{-17}	1.85634×10^{-16}	1.88307×10^{-13}

It suggests that hot carrier stress induces the largest increase of drain current $1/f$ noise amplitude $S_{\rm ID}$, especially at 10 Hz with $S_{\rm ID}$ increasing from 8.88851×10^{-16} to 1.90698×10^{-11}; the rate of change is 214257.4%. Piezoelectric polarization induces the second largest increase of drain current $1/f$ noise amplitude $S_{\rm ID}$, especially at 10Hz with $S_{\rm ID}$ increasing from 8.88851×10^{-16} to 6.6372×10^{-15}; the rate of change is 645.7%. The electrical parameters $\Delta g_{\rm m}/g_{\rm m}$ under hot carrier stress is small with the rate of change being 54.9%. The electrical parameter $\Delta g_{\rm m}/g_{\rm m}$ under piezoelectric stress is the smallest with the rate of change being 11.8%. So that, hot carrier stress induces larger drain current $1/f$ noise degeneration than the piezoelectric polarization effect. Meanwhile, both of their degenerations are more than electronic parameters $\Delta g_{\rm m}/g_{\rm m}$ degeneration for AlGaN/GaN HEMTs. The simulation result of $1/f$ noise after hot carrier stress is too large, because there is no consideration of the interaction between the piezoelectric positively charged defects and hot carrier negatively charged defects.

5. Conclusions

Hot carrier-induced drain current $1/f$ noise in AlGaN/GaN HEMT is studied both theoretically and experimentally. A unified drain current $1/f$ noise model containing piezoelectric polarization effect and hot carrier effect is built, which is based on the fluctuations of the number of carriers in the two-dimensional electron gas (2DEG) channel of AlGaN/GaN HEMT. Experiments show that after hot carrier injection, the drain current $1/f$ noise degradation increases four orders of magnitude; the electrical parameter degradation $\Delta g_{\rm m}/g_{\rm m}$ is 54.9%. The drain current $1/f$ noise degradation reduces one order of magnitude by the piezoelectric polarization effect; the electrical parameter degradation $\Delta g_{\rm m}/g_{\rm m}$ is 11.8%. The simulation results are in good agreement with the experimental results. We obtain that the drain current $1/f$ noise is sensitive to AlGaN/GaN HEMT hot carrier effects and piezoelectric effects. The $1/f$ noise parameter amplitude $S_{\rm ID}$ can act as a useful reliability characterization tool for AlGaN/GaN HEMTs.

References

[1] Labat N, Malbert N, Maneux C, Curutchet A and Grandchamp B 2011 *21st International Conference on Noise and Fluctuations*, 12–16 June, 2011, Toronto, Canada, p. 458

[2] Lü Y J, Lin Z J and Yu Y X , Meng L G, Cao Z F, Luan C B and Wang Z G 2012 *Chin. Phys. B* **21** 097104

[3] Tian W, Yan W Y, Xiong H, Dai J N, Fang Y Y, Wu Z H, Yu C H and Chen C Q 2013 *Chin. Phys. B* **22** 057302

[4] Meneghesso G, Verzellesi V, Danesin F, Rampazzo F, Zanon F, Tazzoli A, Meneghini M and Zanoni E 2008 *IEEE Transactions on Device and Materials Reliability* **8** 332

[5] Balandin A, Cai S, Li R, Wang K L, Rao V R and Viswanathan C R 1998 *IEEE Electron Dev. Lett.* **19** 475

[6] Vertiatchikh A V and Eastman L F 2003 *IEEE Electron Dev. Lett.* **24** 535

[7] Rao H and Bosman G 2009 *J. Appl. Phys.* **106** 1037121

[8] Vitusevich S A, Danylyuk S V and Klein N 2002 *Appl. Phys. Lett.* **80** 2126

[9] Manouchehri F, Valizadeh P and Kabir M Z 2011 *21st International Conference on Noise and Fluctuations*, 12–16 June, 2011 Toronto, Canada, p. 220

[10] Bao J L, Zhuang Y Q and Du L 2005 *Acta Phys. Sin.* **54** 2118 (in Chinese)

[11] Vitusevich S A, Danylyuk S V and Kurakin A M 2006 *J. Appl. Phys.* **99** 0737061

[12] Fang P, Hung K K , Ko P K and Hu C 1990 *Symposium on VLSI Technology*, 4–7 June, 1990, Honolulu, USA, p. 37

[13] Alamo J A and Joh J 2009 *Microelectronics Reliability* **49** 1200

[14] Rao H and Bosman G 2010 *J. Appl. Phys.* **108** 0537071